

# Abundance analysis of the $\lambda$ Bootis stars HD 192640, HD 183324 and HD 84123<sup>\*</sup>

U. Heiter, F. Kupka, E. Paunzen, W.W. Weiss, and M. Gelbmann

Institute for Astronomy, University of Vienna, Türkenschanzstrasse 17, A-1180 Vienna, Austria (last\_name@astro.univie.ac.at)

Received 26 November 1997 / Accepted 22 April 1998

**Abstract.** The classification of  $\lambda$  Bootis stars based on photometric indices or low resolution spectra is not sufficient for a final decision concerning a membership to this group. A detailed spectroscopic investigation is necessary to rule out stars with similar classification spectra but different abundance patterns. Therefore a program on abundance analyses of  $\lambda$  Bootis candidates was established, which makes use of a software package that enables the analysis of high signal-to-noise spectra with large resolution.

In this paper we present the results of the application of these tools on two  $\lambda$  Bootis stars (HD 192640 and HD 183324), for which the derived abundances agree very well with the literature. For a third star (HD 84123), which shows a very low projected rotational velocity, the newly determined abundance pattern confirms its membership to the  $\lambda$  Bootis group.

We also investigated the effect of using several different codes for the calculation of the model atmospheres on the synthetic spectra of the program stars, which span a wide range in effective temperature, gravity and metallicity. The substitution of opacity distribution functions, which were pre-tabulated for metal abundances scaled according to the solar composition, by ones calculated for the individual abundance patterns does not change the synthetic spectra significantly. On the other hand, the derived abundances are sensitive to the treatment of overshooting within the calculation of the convective flux for cool stars.

**Key words:** convection – stars: abundances – stars: chemically peculiar – stars: individual: HD 183324, HD 192640, HD 84123

## 1. Introduction

$\lambda$  Bootis stars are defined as metal-poor Pop I A- to F-type stars, which exhibit solar element abundances for C, N, O and S (Paunzen et al. 1997 and references therein). As has been shown in recent investigations of suspected  $\lambda$  Bootis stars (e.g. Paunzen

et al. 1997), photometric indices in the UV and in the visible, as well as classifications based on flux depressions, spectra of insufficient resolution, etc. suffer from confusion of true  $\lambda$  Bootis stars with non-members of this group, like field horizontal branch stars, shell stars, He-weak stars, etc. In particular, for border-line cases we find many incorrectly attributed  $\lambda$  Bootis memberships. Therefore we regard a sample of most probable  $\lambda$  Bootis stars, which resulted from a survey type investigation of hundreds of  $\lambda$  Bootis candidates using low resolution spectra (Paunzen & Gray 1997). The final decision concerning their membership can be derived only from a detailed spectroscopic investigation, which is very time consuming.

From the beginning of our project (Paunzen et al. 1995) we therefore focused on the development of tools that enable quick, but accurate abundance determinations for  $\lambda$  Bootis stars. They take advantage of modern atomic data bases, like VALD (Piskunov et al. 1995), semi-automatic procedures like AAP (Gelbmann et al. 1997), and high signal-to-noise spectra with sufficiently large spectral resolution in a large spectral range, as are now available with modern echelle spectrographs.

In order to test our routines and procedures, we repeated the abundance analysis for the two  $\lambda$  Bootis stars HD 192640 and HD 183324, for which independent investigations are found in the literature (Stürenburg 1993, Venn & Lambert 1990). One aspect of this paper is to compare our results with earlier determinations and to discuss disagreements. We derive  $T_{\text{eff}}$  and  $\log g$  spectroscopically and do not have to rely on the calibration of photometric indices. In addition, the number of elements for which abundances are determined, or at least for which upper limits can be given, has been increased. As the comparison with published results demonstrates the reliability of our methods we continue to examine high-resolution-spectra of further  $\lambda$  Bootis stars, which up to now have not been investigated in detail. In this paper we present the results of the abundance analysis of one of the coolest  $\lambda$  Bootis stars, HD 84123. We use these results as well as the new Hipparcos data to deduce the evolutionary status of the program stars and discuss the significance of the derived abundances for the theories that propose an explanation of the  $\lambda$  Bootis phenomenon.

Several members of the  $\lambda$  Bootis group exhibit  $\delta$  Scuti like oscillations. HD 192640 was the first  $\lambda$  Bootis star for which such pulsation was reported (Gies & Percy 1977). New obser-

---

Send offprint requests to: U. Heiter

<sup>\*</sup> Based on observations obtained at the Observatoire de Haute Provence, the Osservatorio Astronomico di Padua-Asiago and with the Hipparcos satellite

Correspondence to: U. Heiter

vations by Paunzen & Handler (1996) indicated two periods of 38 and 43 minutes with amplitudes of 26 and 13 mmag in Strömgren *b*. HD 183324 is pulsating with a period of 30 minutes and an amplitude of 4 mmag in Strömgren *v* (Kuschnig et al. 1994). HD 84123 is constant with an upper limit of 3 mmag in Strömgren *b* (Paunzen et al. 1998b). Line profile deformations due to nonradial pulsation in these stars have not been taken into account in the present work.

With the aim of reducing some of the problems associated with the calculations that are involved in abundance analyses we study the impact of self-consistent models for stellar atmospheres on the atmosphere structure, the surface flux and the derived abundances. The first part of this work deals with the comparison of model atmospheres calculated with solar scaled line opacity tables (Kurucz 1993) and atmospheres computed for the particular abundance pattern of  $\lambda$  Bootis stars. The latter became available when opacity distribution functions for arbitrary chemical compositions could be computed in our group (Piskunov & Kupka 1998). The second part concerns the calculation of the convective flux in the  $\lambda$  Bootis atmospheres. We look at the effects on synthetic spectra of the CM-model (Canuto & Mazzitelli 1991) as an alternative to mixing length theory, and various solutions for the treatment of overshooting.

## 2. Observations

The spectra of HD 192640 and HD 183324 were obtained in June and August 1994 at the Observatoire de Haute Provence by M. Gelbmann and R. Kuschnig. The observations with the Aurelie spectrograph mounted on the 1.52 m telescope cover the spectral ranges from 3800 Å to 5300 Å and 5800 Å to 6000 Å, and for HD 192640 also from 5900 Å to 6280 Å and 7050 Å to 7230 Å. The spectral resolution for these stars is about 20000 with a dispersion of 8 Å mm<sup>-1</sup>. The spectra show a typical signal to noise ratio of 200.

For HD 84123 UH obtained two spectra with the echelle spectrograph of the 1.82 m telescope of the Osservatorio Astronomico di Padua-Asiago in March 1995 and February 1997. They range from 4000 Å to 7200 Å with a resolution of about 30000 and a dispersion of 5 Å mm<sup>-1</sup> in the blue and 10 Å mm<sup>-1</sup> at 6000 Å. The signal to noise ratio of these spectra is between 100 and 200.

The reductions of these observations were done with the onedspec and echelle packages of NOAO IRAF (Willmarth & Barnes 1994).

## 3. Stellar atmosphere parameters

The parameters of the model atmospheres used to calculate the synthetic spectra have been derived iteratively by determining ‘line’ abundances (see Sect. 4) for single iron lines. The correct value for the microturbulent velocity  $\xi$  renders the ‘line’ abundance independent of the equivalent width. For the determination of  $\log g$  the difference in ‘line’ abundance between neutral and ionized lines must be as small as possible. Finally, a zero gradient in a ‘line’ abundance versus lower energy level diagram

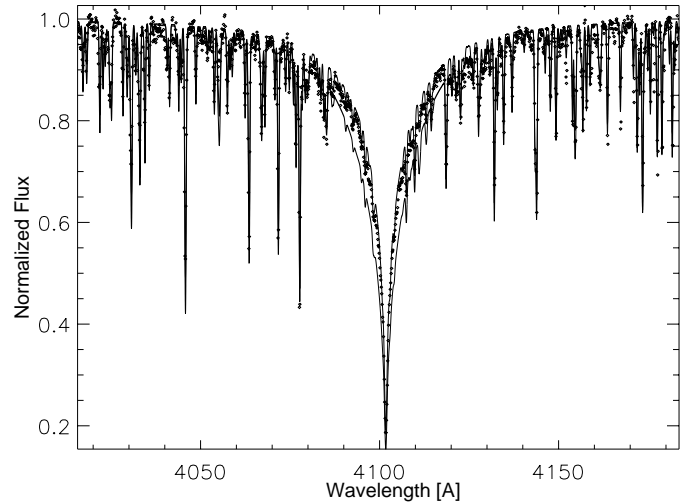


**Fig. 1.** H $\delta$  line profiles for HD 84123. Observations (diamonds) and calculations (upper solid line (6600,3.8), lower solid line (7000,3.2)).

**Table 1.** Atmospheric parameters for the three stars. Errors in parentheses are in units of the last significant digit. For the choice of the metallicity  $[Z]$  see Sect. 3.

star HD	$T_{\text{eff}}$ [K]	$\log g$	$\xi$ [km s <sup>-1</sup> ]	$[Z]$	$v \sin i$ [km s <sup>-1</sup> ]
84123	6800(200)	3.5(3)	3.0(5)	-1.0	15(5)
183324	9300(200)	4.3(3)	3.0(5)	-1.5	90(10)
192640	7800(200)	4.0(3)	3.0(5)	-2.0	80(10)

is used to determine the effective temperature  $T_{\text{eff}}$ . The model atmospheres were calculated with ATLAS9 (Kurucz 1993) with scaled solar abundances, using pretabulated opacity distribution functions (ODFs) with a metallicity  $[Z]$  as close as possible to the iron abundances. The atomic transition parameters for spectrum synthesis have been taken from the Vienna Atomic Line Database VALD (Piskunov et al. 1995). Every step of this procedure – calculating the model atmosphere, generating a line list, synthesizing the lines and plotting abundance diagrams – has been performed with the semi-automatic tool AAP (Abundance Analysis Procedure, see Gelbmann et al. 1997).

The rotational velocity  $v \sin i$  was estimated with the program ROTATE (Piskunov 1992), which plots observed and synthetic spectra simultaneously and convolves the latter with the instrumental and rotational profiles.

The final parameters for the three investigated stars are listed in Table 1. These results were used to determine the abundances of all other elements for which suitable lines were found in the observed spectral range.

A test of the parameters listed in Table 1 has been made by calculating synthetic Hydrogen line profiles for a grid of model atmospheres with  $T_{\text{eff}}$  and  $\log g$  varied according to the given errors. The observed H $\gamma$  and H $\delta$  lines have been normalized using classification spectra provided by E. Paunzen (private communication). They fall in between the weakest and strongest of the synthetic profiles and therefore confirm the above determined parameters. For HD 84123, the H $\delta$  profiles calculated

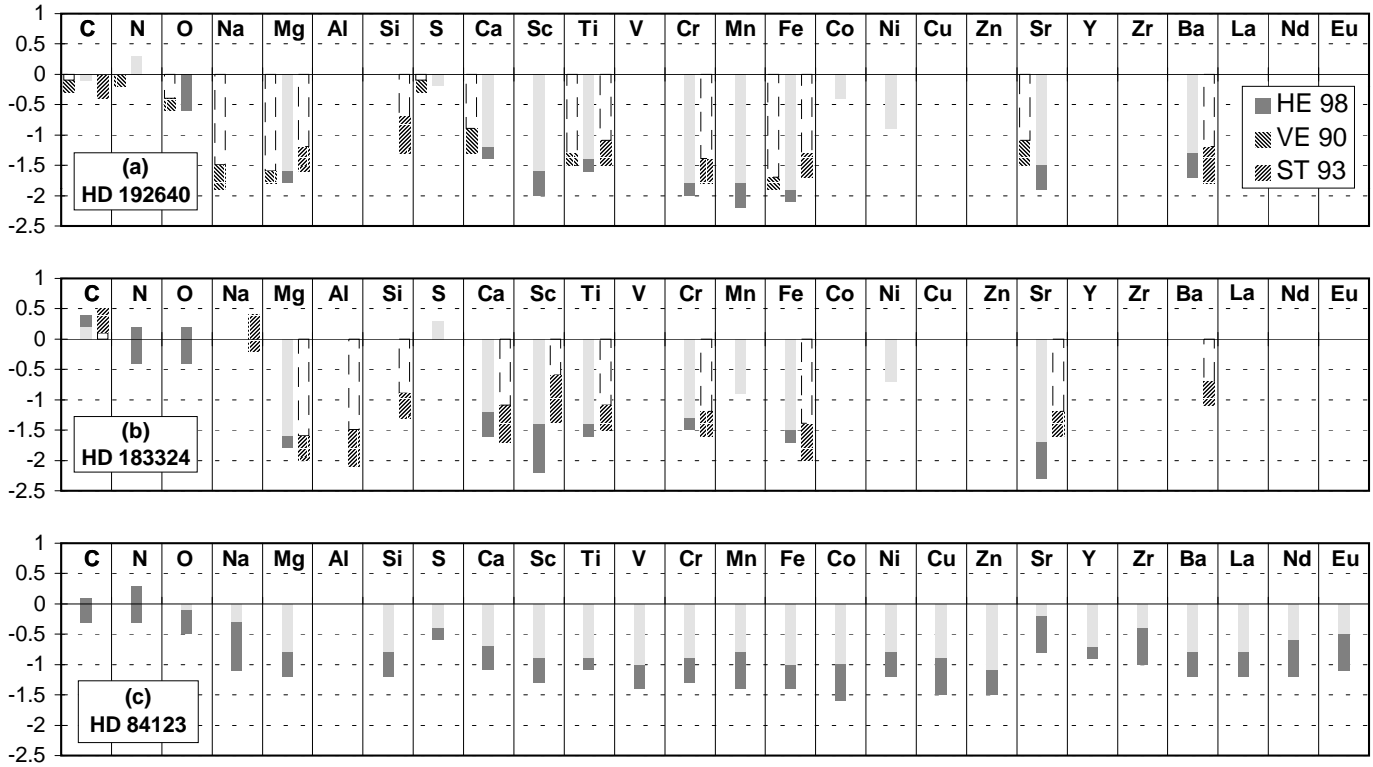


Fig. 2. Logarithm of abundances of the three  $\lambda$  Bootis stars with estimated error ranges indicated in dark grey.

**Table 2.** Abundances of the three stars. For each element  $X$  we list  $\log \left( \frac{N_X}{N_{\text{tot}}} \right) - \log \left( \frac{N_X}{N_{\text{tot}}} \right)_{\odot}$  where the solar abundances are taken from Anders & Grevesse (1989). The columns containing the numbers of lines per element for two ionisation stages are labeled No. Errors in parantheses are in units of the last significant digit.

Element	No.	HD 192640	No.	HD 183324	No.	HD 84123
C	4/0	< -0.1	6/0	+0.3(1)	9/0	-0.1(2)
N	1/0	< +0.3	1/0	-0.1	1/0	+0.0
O	1/0	-0.3	1/0	-0.1	7/0	-0.3(2)
Na					10/0	-0.7(4)
Mg	2/2	-1.7(1)	2/2	-1.7(1)	7/1	-1.0(2)
Si					3/3	-1.0(2)
S	4/0	< -0.2	2/0	< +0.3	10/0	-0.5(1)
Ca	6/1	-1.3(1)	1/1	-1.4(2)	35/2	-0.9(2)
Sc	0/2	-1.8(2)	0/1	-1.8	0/10	-1.1(2)
Ti	0/11	-1.5(1)	0/6	-1.5(1)	4/33	-1.0(1)
V					2/5	-1.2(2)
Cr	4/1	-1.9(1)	2/2	-1.4(1)	11/17	-1.1(2)
Mn	3/0	-2.0(2)	1/0	< -0.9	14/0	-1.1(3)
Fe	25/13	-2.0(1)	7/7	-1.6(1)	179/32	-1.2(2)
Co	3/0	< -0.4			2/0	-1.3(3)
Ni	6/0	< -0.9	0/2	< -0.7	20/0	-1.0(2)
Cu					2/0	-1.2(3)
Zn					3/0	-1.3(2)
Sr	0/2	-1.7(2)	0/2	-2.0(3)	0/3	-0.5(3)
Y					0/7	-0.8(1)
Zr					0/9	-0.7(3)
Ba	0/2	-1.5(2)			0/6	-1.0(2)
La					0/4	-1.0(2)
Nd					0/1	-0.9
Eu					0/1	-0.8

with  $(T_{\text{eff}}, \log g) = (6600, 3.8)$  and  $(7000, 3.2)$ , together with the observations, are displayed in Fig. 1.

Measurements of the circular polarization in  $H_{\beta}$  of ten  $\lambda$  Bootis stars showed that the magnetic fields of these stars are smaller than 300 G (Bohlender & Landstreet 1990). In the course of the present work we found that the iron ‘line’ abundances are independent of the effective Landé factors within the error ranges. This indicates that the lines are not broadened by a magnetic field larger than 1 kG.

#### 4. Abundances

Every “unblended” line in the examined spectral regions with a minimal central line depth of 0.1 (before convolution with instrumental profile and rotational kernels) was synthesized with the models described above. The criteria for a line to be “unblended” require that no other line with a line depth greater than 30 % of that of the examined line is found inside a wavelength window of 3 Å around the central wavelength of the examined line. The abundance of the considered element was chosen such that the profiles of the synthetic and observed lines matched as close as possible. This procedure has partially been carried out with the autofit option of the AAP program. The abundance of an individual element was derived by averaging all ‘line’ abundances. Table 2 shows the resulting abundances for the three  $\lambda$  Bootis stars relative to the sun. The errors for elements for which more than one line has been used are the standard deviations of the means and are given in parentheses.

For several elements the observed spectrum showed only very weak lines which could hardly be distinguished from noise. In this case the abundance for the synthetic line was increased until the line depth was greater than the noise level, which gave an estimate for the upper abundance limit. In Table 2 these cases are indicated by a ‘<’ sign before the abundance values.

All line calculations were made using the LTE approach. Recent calculations found in the literature have shown that non-LTE effects on the element abundances are of minor importance for the parameters and lines used in the present work. A theoretical study for effective temperatures between 7000 and 12000 K has been made by Rentzsch-Holm (1996). The non-LTE abundance corrections for Fe I are about +0.2 dex, for Fe II there are no differences between lines in LTE and non-LTE. For Carbon, the non-LTE effects are between  $-0.2$  and  $0$  dex, if the equivalent widths of the lines are lower than 100 mÅ. Stürenburg (1993) has calculated non-LTE abundances for several elements in HD 183324 and HD 192640. The absolute values of the resulting non-LTE corrections are lower than 0.2 dex for all of the examined elements, and hence are comparable to the abundance errors. For stars with an effective temperature of 6500 K, detailed statistical equilibrium calculations by Mashonkina et al. (1996), Belyakova & Mashonkina (1996) and Mashonkina & Bikmaev (1996) show that non-LTE effects for Mg I, Sr II and Ba II are lower than 0.1 dex. From the above statements one can conclude that the overall abundance pattern of  $\lambda$  Bootis stars is not changed significantly, when non-LTE effects are taken into account.

**Table 3.** Photometrically derived parameters of HD 192640 and HD 183324.

	HD 192640		HD 183324
	VE90	ST93	ST93
$T_{\text{eff}}[\text{K}]$	8100	7990	9260
$\log g$	4.0	4.0	4.2

##### 4.1. HD 192640

The first of the investigated objects, 29 Cygni, is one of the early members of the  $\lambda$  Bootis group. It was already analyzed by Venn & Lambert (1990, VE90) and Stürenburg (1993, ST93). Their model atmospheres were based on atmospheric parameters that resulted from a calibration of photometric indices in the Strömgren system. They are listed in Table 3 and agree with the parameters used in this work within the error range given in Table 1. The values for  $v \sin i$  and  $\xi$  that have been inferred from line profile and equivalent width measurements are identical in all three papers. In the spectral region covered by our observations we found about 100 useful spectral lines and could therefore detect 15 elements. A detailed description of the abundance analysis as well as an atlas of the spectrum of this star can be found in Heiter (1996). With an underabundance of up to  $-2$  dex with respect to the sun this star is the most metal deficient in our sample. The abundance values of the previous studies – for the comparison with ST93 we used his LTE values – could in general be confirmed. In addition, the list of elements with determined abundances has been extended.

The abundance pattern of HD 192640 is illustrated in Fig. 2 (a). For comparison we also plot the results of VE90 and ST93. The light elements C, N, O and S are practically solar abundant, whereas the abundances of all other elements are lower than  $-1$  dex in comparison with their solar value. The individual values agree within the error ranges with the results of VE90. The abundance values of ST93 are somewhat larger, but they accord within the errors, except for iron, where the difference is 0.5 dex.

##### 4.2. HD 183324

The second program star, 35 Aquilae, is located at the hot end of the area that is occupied by the  $\lambda$  Bootis stars in the HR diagram. For this reason its spectrum showed only about 50 metal lines and we could detect 13 elements. This star is also included in the list of 15 objects analyzed by ST93. Its abundance pattern is represented in Fig. 2 (b) and is similar to that of HD 192640. The abundances agree very well with the literature, only the abundance values of Sr show a noticeable difference of 0.6 dex. Since the Sr lines are very weak in this star the error ranges have probably been underestimated and the difference may not be significant.

### 4.3. HD 84123

The abundance analysis of the coolest star is based on about 450 lines of 25 elements. It is less underabundant than the other two stars as can be seen from Fig. 2 (c). Since the analysis of this star is based on an echelle spectrum with somewhat lower signal to noise ratio and the level of the continuum is more uncertain the internal errors of the abundances are in general larger than for the other two stars. This is the only star for which we could derive the abundance of Na. When compared with published results for the other two stars it seems that the role of this element in the atmosphere of  $\lambda$  Bootis stars cannot be specified uniquely. Further investigations are needed to throw more light on this problem. Note that this is one of the few  $\lambda$  Bootis stars with a low projected rotational velocity, which could now be confirmed by high resolution spectroscopy. Five other  $\lambda$  Bootis stars with  $v \sin i$  lower than  $50 \text{ km s}^{-1}$  can be found in Paunzen & Gray (1997) and Paunzen et al. (1998a).

### 4.4. Evolutionary status of our program stars

In order to derive the evolutionary status for all three program stars, we have used the Hipparcos data as well as the (spectroscopically) determined effective temperatures from Table 1. Since the origin of the  $\lambda$  Bootis phenomenon is still controversial, an age determination could help to decide between the two proposed theories – mass loss with diffusion (Michaud & Charland 1986), which leads to underabundances only for stars with slow equatorial rotation, and the accretion theory (Venn & Lambert 1990). A recent paper (Paunzen 1997) established at least nine members of the  $\lambda$  Bootis group as *very close to the Main Sequence* (age  $\approx 10^7$  years) supporting the predictions of the accretion theory.

With the Hipparcos parallaxes,  $M_V$  values have been determined and the bolometric corrections (from Schmidt-Kaler 1982) were added. Using  $M_{\text{Bol}}(\odot) = 4.75$  given by Cayrel de Strobel (1996), we have calculated  $\log L/L_\odot$  as listed in Table 4.

The evolutionary tracks for the Main Sequence were taken from Claret (1995, “MS”) whereas the Pre-Main Sequence models are from Palla & Stahler (1993, “PMS”). Table 4 lists the derived masses and ages of all program stars for both models.

It is immediately evident that HD 183324 is *very close to the Main Sequence* ( $M \approx 2.1 M_\odot$ ), in accordance with the accretion theory. The age determinations for the other two stars are not unique within the Pre- and Main Sequence models. That is, they have either proceeded half way from the “birthline”, at which the accretion onto the protostar ends instantaneously, to the ZAMS, or are in the middle (HD 192640) or at the end (HD 84123) of their Main Sequence lifetimes. We are therefore not able to conclude if these stars are indeed young objects.

We note that, for the first time, the abundance of Zn was determined for a  $\lambda$  Bootis star (HD 84123, Table 2). If accretion of interstellar gas, depleted of elements which have condensed into dust grains, takes place, the Zn abundance should resemble the abundances of the light elements (C, N, O and S) because

**Table 4.** Derived masses and ages of our program stars. The zeropoints for  $\log t_{\text{PMS}}$  and  $\log t_{\text{MS}}$  are the birthline (see text) and the ZAMS, respectively. Errors in parantheses are in units of the last significant digit.

	HD 84123	HD 183324	HD 192640
$V$ [mag]	6.87	5.77	4.95
$M_{\text{Bol}}$ [mag]	1.52(22)	1.70(11)	1.74(5)
$\log L/L_\odot$	1.29(8)	1.22(4)	1.20(2)
$\mathcal{M}_{\text{PMS}}$ [ $M_\odot$ ]	2.0	2.1	1.9
$\log t_{\text{PMS}}$	6.65	6.90	6.75
$\mathcal{M}_{\text{MS}}$ [ $M_\odot$ ]	1.9	2.2	1.9
$\log t_{\text{MS}}$	8.95	7.00	8.60

of its similarly high condensation temperature (Van Winckel et al. 1992). But Zn is depleted like the Fe-peak elements in this star, and since the projected rotational velocity is very low, the diffusion/mass loss theory seems to be supported.

## 5. Selfconsistent $\lambda$ Bootis star atmospheres

### 5.1. Individual ODFs

Up to now abundance analyses of B – K stars have mostly been performed with model atmospheres that allowed for line opacities by means of opacity distribution functions (ODFs) tabulated for certain metal abundances scaled according to solar composition. The recent development of a program that enables the calculation of ODFs for arbitrary metal abundances showed that for stars with overabundances of Si, e.g., the  $T(\tau)$ -relation and therefore the synthetic spectrum is changed significantly (Piskunov & Kupka 1998).

In this context one can question if this result would also be important for the metal deficient  $\lambda$  Bootis stars. Consequently, we calculated ODFs for the three investigated stars using the metal abundances given in Table 2. The relative difference in the  $T(\tau)$ -relations of the model atmospheres obtained with these individual ODFs ( $\frac{T_{\text{ODF}} - T_{\text{scaled}}}{T_{\text{scaled}}}$ ) is lower than three percent for all three stars.

This small difference has only a very small influence on the synthetic spectra. The difference in line depths between spectra with individual and scaled ODFs is smaller than 0.4 % over the entire examined spectral range for HD 192640 (0.3 % for HD 183324), only in the centers of the Calcium H and K lines it reaches 0.8 %, which is illustrated in Fig. 3. The differences between the surface fluxes emitted from the modified and the scaled model atmospheres are represented in Fig. 4. Except for the centers of the Hydrogen Balmer lines, which are treated in different ways in the two opacity codes, and the Balmer jump, for which a more accurate calculation will be possible in a forthcoming version of the opacity program, they are lower than one percent in the optical region for all three stars.

### 5.2. Convection modeling

Another issue of concern in modeling stellar atmospheres is the calculation of the convective flux. Recently, a few suggestions

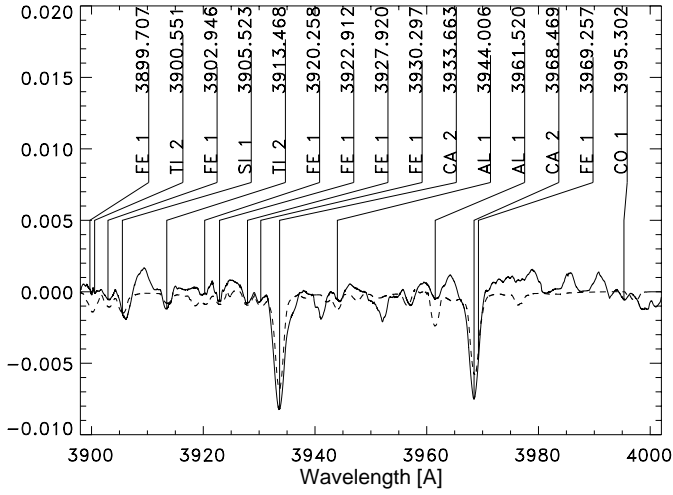


**Fig. 3.** Difference between normalized synthetic spectra with individual and solar scaled ODFs. The solid and dashed lines represent HD 192640 and HD 183324 respectively.

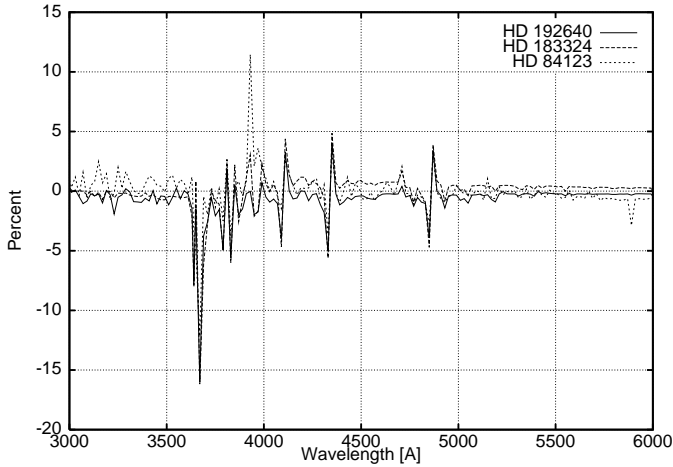


**Fig. 4.** Relative difference of ODF and solar scaled fluxes ( $\frac{F_{\text{ODF}} - F_{\text{scaled}}}{F_{\text{scaled}}}$ ).

were proposed to improve the classical mixing length theory used in the original ATLAS9 program. The most prominent is the CM model (Canuto & Mazzitelli 1991) which is based on turbulence theory and has been implemented in the ATLAS9 program (Kupka 1996, see also Smalley & Kupka 1997). In this section we compare model atmospheres and fluxes of metal poor stars calculated with four different versions of ATLAS9. The first is the original program published on CDROM 13 by Kurucz (1993) without any changes (MLT). Second, since this treatment of overshooting is not reliable (Castelli et al. 1997), we deleted this part of the program (NO). Third, Castelli (1996) presented a correction of an inconsistency in the original treatment of overshooting in Kurucz (1993) (OVOK). Finally, we regard the CM model.

Because of the high effective temperature of HD 183324 the contribution of convection to the total flux is negligible and the  $T(\tau)$ -relation is the same when calculated with MLT or CM. Therefore this star will not be discussed further in this section.

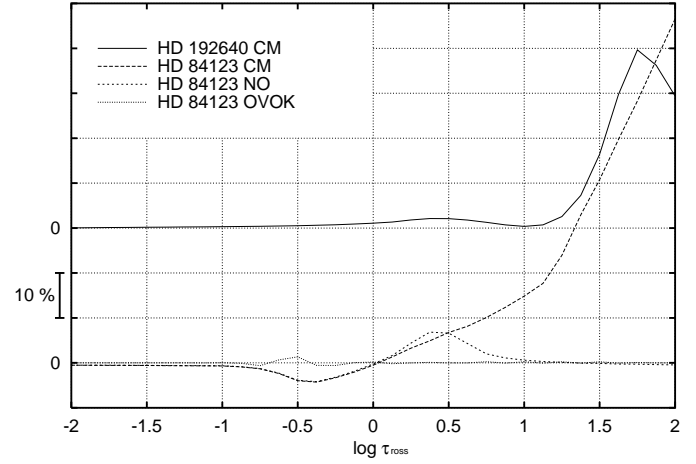


**Fig. 5.** Difference of the temperature structures between various convection models and MLT ( $\frac{T_{\text{CONV}} - T_{\text{MLT}}}{T_{\text{MLT}}}$ ).

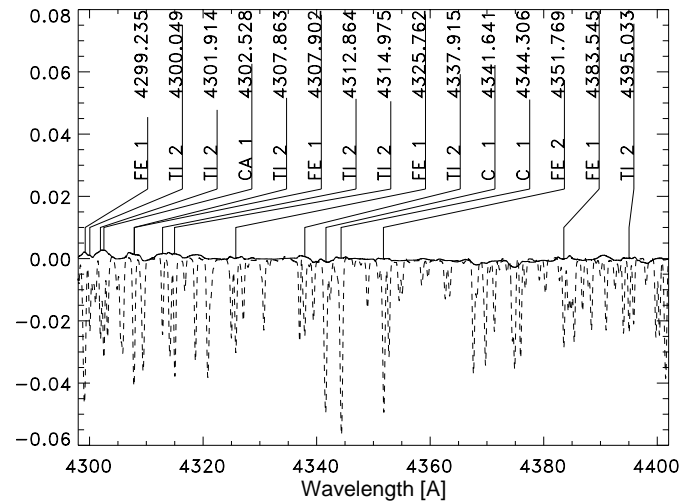


**Fig. 6.** Difference between normalized synthetic spectra calculated with CM and MLT models. The solid and dashed lines represent HD 192640 and HD 84123 respectively.

In HD 192640 where convection is more important one can see a difference in the  $T(\tau)$ -relations of CM and MLT of up to 40 % for  $\log \tau_{\text{ross}} \geq 1$ . However, in the line forming region ( $0 < \log \tau_{\text{ross}} < 1$ ) the difference is smaller than two percent and thus not visible in the spectrum.

The situation is more dramatic for HD 84123, which is the coolest of the three stars. The remarkable difference between the  $T(\tau)$ -relations of the CM and MLT models is obvious from Fig. 5. The NO model leads to an enhancement in the line forming region of the same order of magnitude as the CM model but is similar to the MLT model for  $\log \tau_{\text{ross}} \geq 0.6$ . The model with the overshooting correction (OVOK) practically has the same  $T(\tau)$ -relation as the model with the original overshooting treatment (MLT).

The consequences of these changes in the atmospheric structures of HD 192640 and HD 84123 on the synthetic spectra are illustrated in Fig. 6. For HD 192640 the differences between

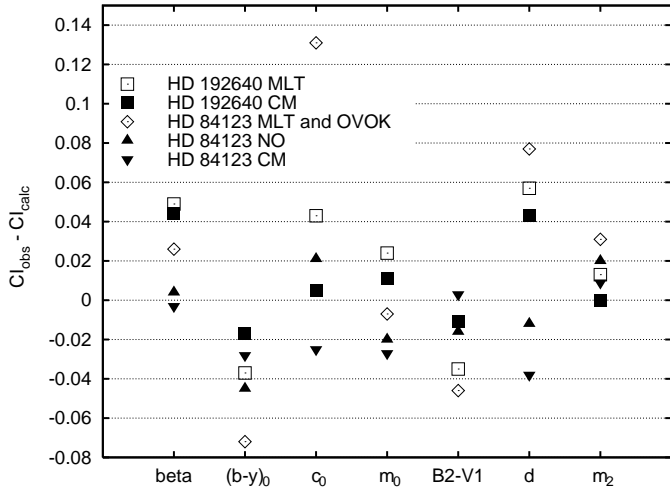


**Fig. 7.** Differences of color indices in the Strömgren and Geneva systems between various model atmospheres and observations.

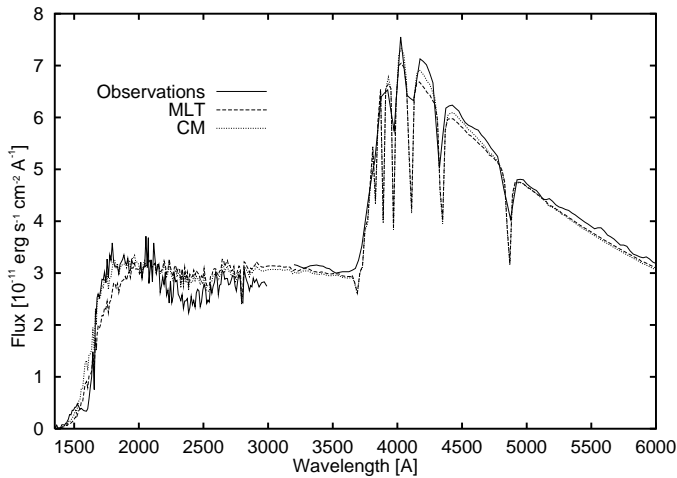


**Fig. 8.** Comparison of synthetic surface fluxes with IUE and optical observations for HD 192640.

**Table 5.** Abundances  $\log \frac{N_X}{N_{\text{tot}}}$  of some elements (X) for HD 84123 and MLT and CM convection models. Errors in parantheses are in units of the last significant digit.

Element	C	Ti	Cr	Fe
MLT	-3.5(2)	-8.0(1)	-7.4(2)	-5.5(2)
CM	-3.6(2)	-8.1(1)	-7.5(2)	-5.6(2)

synthetic spectra based on model atmospheres with CM and MLT convection treatment is below the observational errors and does not show any noticeable trend. The increase in linedepth of up to five percent for the CM model of HD 84123 results in an abundance decrement of 0.1 dex compared to the MLT model, as listed in Table 5. For Fe, the abundance determined with the OVOK model equals that of the MLT model, and calculations based on the model without overshooting result in the same abundance as that for the CM model. Since the effect is the same for lines of different elements and ionisation stages, the determination of the atmospheric parameters does not have to

**Table 6.** Color indices observed in the Strömgren and Geneva systems for the two cooler program stars.

HD	$(b-y)_0$	$c_0$	$m_0$	$\beta$
84123	0.192	0.735	0.087	2.713
192640	0.101	0.927	0.157	2.833
	$B2-V1$	$d$	$m_2$	
84123	0.117	1.142	-0.542	
192640	-0.013	1.367	-0.538	

be repeated. Furthermore, the abundance changes lie within the estimated errors. Nevertheless we have used the CM model to derive the abundances of HD 84123 given in Table 2 because the abundance deviation is systematic. In addition, the synthetic colors calculated with the CM model show a smaller difference to the observed colors for A and F type stars than with models based on the OVOK or NO treatment of convection (see Smalley & Kupka 1997), which is also true for our program stars, except for the  $m_0$  index (Fig. 7). The observed colors are listed in Table 6. The dereddened Strömgren colors and indices have been derived using the procedure of Olsen (1988).

An inspection of the surface fluxes calculated with various convection approaches reveals a significant enhancement in the UV flux of the CM model. For HD 192640 the spectra SWP44622L and LWP23062L have been extracted from the IUE Final Archive by E. Solano. In addition, observed fluxes from 3200 Å to 6000 Å have been taken from Burnashev (1985). A comparison shows that the CM flux of HD 192640 seems to represent the observations better than the flux of the MLT model atmosphere. In particular, the steep decrease in the UV flux from 1800 Å to 1400 Å can only be modeled with CM theory (see Fig. 8). An exception is the broad absorption feature at 1600 Å which characterizes the spectra of  $\lambda$  Bootis stars and was identified as a pseudo-molecular absorption feature of  $L_\alpha$  by Holweger et al. (1994). This feature cannot be reproduced by the two models. No spectrophotometric observations were available for HD 84123 but in Fig. 9 we compare the synthetic UV fluxes for this star with measurements obtained by the TD1 satellite (Thompson et al. 1978). Although there is a large discrepancy between calculations and observations shortward of 2600 Å the convection models without overshooting shift the fluxes to smaller differences compared to the observations.

## 6. Conclusions

In this paper we have analyzed the chemical composition of three  $\lambda$  Bootis stars, where for two stars abundances of some elements have been published by other authors. The excellent agreement between the previous and the new results confirms the reliability of our new software package for abundance determinations. For HD 192640 the iron abundances found by Stürenburg (1993) disagree by 0.5 dex. Since the current analysis yields an underabundance of -2 dex, which is consistent with VE90 we suggest this value to represent the actual iron deficiency of HD 192640. In addition, we could derive abundances of further elements for the first two stars.

We applied our tools to a cool, sharp lined  $\lambda$  Bootis star which had been detected during a spectroscopic survey (Paunzen & Gray 1997). The underabundances of all elements except C,N,O and S of about  $-1$  dex confirm the membership of this star to the  $\lambda$  Bootis group.

In this context we discuss the critical problem of the confusion of  $\lambda$  Bootis stars with groups of stars showing similar classification spectra. In particular, the cool end of the  $\lambda$  Bootis region in the HR diagram overlaps with the region of the field blue stragglers (Andrievsky et al. 1995), where some members have similar atmospheric parameters as HD 84123 (Fig. 10). But these stars exhibit completely different abundance patterns in comparison with  $\lambda$  Bootis stars, with a mean underabundance of  $-0.3$  dex. On the other hand, Corbally & Gray (1996) and Gray et al. (1996) found several field horizontal branch candidates (FHB) with similar spectral characteristics as  $\lambda$  Bootis stars. Recent abundance analyses also give underabundances of heavy elements for FHB stars comparable to  $\lambda$  Bootis stars, that is  $-1.0$  to  $-2.5$  dex (Adelman & Philip 1996). However, the so-called “FHB  $\lambda$  Bootis stars” are clearly distinct from the Population I  $\lambda$  Bootis stars in that they have lower  $\log g$  values and therefore larger  $c_1$  indices (see Fig. 10). HD 84123 has been suggested to be a member of the FHB stars (Paunzen & Gray 1997) but the  $c_1$  index does not confirm this classification.

Using Hipparcos parallaxes we estimated the absolute magnitudes of our program stars. We could establish the evolutionary status of at least one star, HD 183324, to be at the Zero Age Main Sequence, which would favor the accretion theory (Venn & Lambert 1990) for  $\lambda$  Bootis stars. The other two program stars are not located at the ZAMS, but no conclusion concerning their Pre Main Sequence or Main Sequence evolutionary status is possible.

We also investigated the impact of different model atmospheres on the abundance analysis. We found that the calculation of ODFs for individual  $\lambda$  Bootis abundance patterns is not necessary because the synthetic spectra are basically identical to spectra calculated with model atmospheres based on ODFs for abundances ratios similar to that of the sun.

Another problem we have dealt with is the description of convection in stellar atmospheres, in particular the treatment of overshooting. For  $\lambda$  Bootis stars, convection plays an important role only for temperatures below 7000 K. MLT models without overshooting or the CM models yield slightly larger underabundances than the two models with overshooting. Nevertheless,  $T_{\text{eff}}$  and  $\log g$  remain independent of the convection model.

As a conclusion it seems to be sufficient to determine the abundances for  $\lambda$  Bootis stars with Kurucz model atmospheres based on scaled solar composition. The effects of individual ODFs and the treatment of convection are only marginal. Since  $\lambda$  Bootis stars very probably have a global solar composition (Paunzen et al. 1998b), we are left with a vertical stratification to obtain the surface abundances. This stratification can be induced by either of the proposed explanations of the  $\lambda$  Bootis phenomenon (Michaud & Charland 1986, Turcotte & Charbonneau 1993), and its influence on the atmospheric structure and further on abundance determination still has to be investigated.

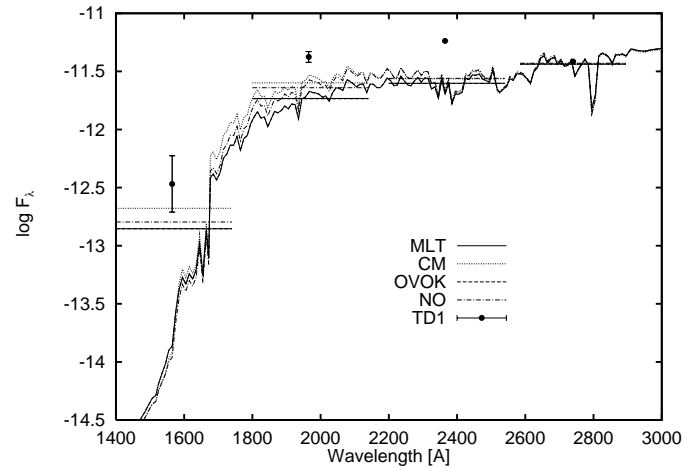


**Fig. 9.** Comparison of synthetic surface fluxes ( $\text{erg s}^{-1} \text{cm}^{-2} \text{\AA}^{-1}$ ) with TD1 observations for HD 84123. The position of the horizontal lines represents the synthetic broadband fluxes calculated over the wavelength range indicated by the length of the lines.

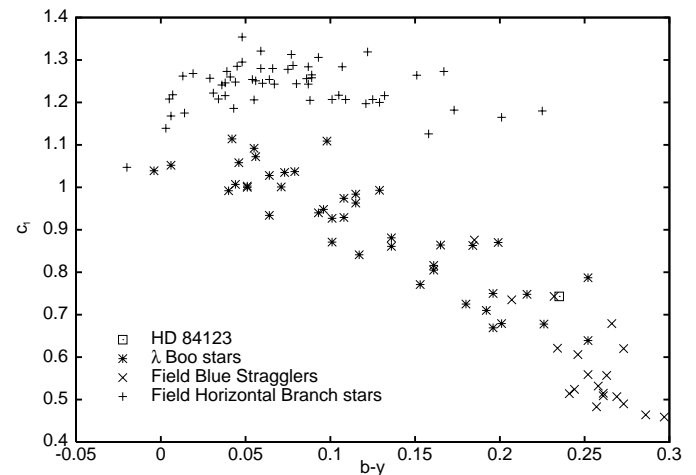


**Fig. 10.** Observational HR diagram. Color indices have not been dereddened.

**Acknowledgements.** This investigation was carried out within the working group *Asteroseismology-AMS* with funding from the Fonds zur Förderung der wissenschaftlichen Forschung (project S7303-AST). UH acknowledges partial financial support by the Austrian Zentrum für Auslandsstudien. We thank R. Kuschnig and Dr. E. Solano for providing a part of the observations and the IUE spectra, respectively. Use was made of the Simbad database, operated at CDS, Strasbourg, France.

## References

- Adelman S.J., Philip A.G.D., 1996, MNRAS 280, 285  
 Anders E., Grevesse N., 1989, Geochimica et Cosmochimica Acta 53, 197  
 Andrievsky S.M., Chernyshova I.V., Ivashchenko O.V., 1995, A&A 297, 356  
 Belyakova E.V., Mashonkina L.I., 1996, ARep 41, 530  
 Bohlender D.A., Landstreet J.D., 1990, MNRAS 247, 606  
 Burnashev V.I., 1985, Abast. Astrofiz. Obs. Bull. 59, 83  
 Canuto V.M., Mazzitelli I., 1991, ApJ 370, 295



- Castelli F., 1996, in proc. “Model Atmospheres and Spectrum Synthesis”, S.J. Adelman, F. Kupka & W.W. Weiss eds., ASP Conf.Ser. 108, p.85
- Castelli F., Gratton R., Kurucz R.L., 1997, A&A 318, 841; *Erratum*: 1997, A&A 324, 432
- Cayrel de Strobel G., 1996, A&AR 7, 243
- Claret A., 1995, A&AS 109, 441
- Corbally C.J., Gray R.O., 1996, AJ 112, 2286
- Gelbmann M., Kupka F., Weiss W.W., Mathys G., 1997, A&A 319, 630; *Erratum*: 1997, A&A 322, 1026
- Gies R., Percy J.R., 1977, AJ 82, 166
- Gray R.O., Corbally C.J., Philip A.G.D., 1996, AJ 112, 2291
- Heiter U., 1996, Master Thesis, Univ. Vienna
- Holweger H., Koester D., Allard N.F., 1994, A&A 290, L21
- Kupka F., 1996, in proc. “Stellar Surface Structure”, IAU Symp. 176, K.G.Strassmeier & J.L.Linsky eds., Vienna, p.557
- Kurucz R.L., 1993, CD-ROM 1-23, Smithsonian Astrophysical Observatory
- Kuschnig R., Paunzen E., Weiss W.W., 1994, IBVS 4070
- Mashonkina L.I., Bikmaev I.F., 1996, ARep 40, 94
- Mashonkina L.I., Shimanskaya N.N., Sakhbullin N.A., 1996, ARep 40, 187
- Michaud G., Charland Y., 1986, ApJ 311, 326
- Olsen E.H., 1988 A&A 189, 173
- Palla F., Stahler S.W., 1993, ApJ 418, 414
- Paunzen E., 1997, A&A 326, L29
- Paunzen E., Gray R.O., 1997, A&AS 126, 407
- Paunzen E., Handler G., 1996, IBVS 4318
- Paunzen E., Gelbmann M., Heiter U., Kupka F., Kuschnig R., Weiss W.W., 1995, in proc. “Astrophysical Applications of Stellar Pulsation”, IAU Coll. 155, R.S. Stobie & P.A. Whitelock, eds., ASP Conf.Ser. Vol. 83, p.315
- Paunzen E., Weiss W.W., Heiter U., North P., 1997, A&AS 123, 93
- Paunzen E., Heiter U., Handler G., Garrido R., Solano E., Weiss W.W., Gelbmann M., 1998a, A&A 329, 155
- Paunzen E., Weiss W.W., Kuschnig R., Handler G., Strassmeier K.G., North P., Solano E., Gelbmann M., Künzli M., Garrido R., 1998b, A&A, in press
- Piskunov N.E., 1992, in proc. “Stellar magnetism”, Nauka, St. Petersburg, p.92
- Piskunov N.E., Kupka F., 1998, A&A, submitted
- Piskunov N.E., Kupka F., Ryabchikova T.A., Weiss W.W., Jeffery C.S., 1995, A&AS 112, 525
- Rentzsch-Holm I., 1996, A&A 312, 966
- Schmidt-Kaler Th., 1982, in: Landolt-Börnstein New Series, group VI, vol. 2b, p. 453
- Smalley B., Kupka F., 1997, A&A 328, 349
- Stürenburg S., 1993, A&A 277, 139
- Thompson G.I., Nandy K., Jamar C., Monfils A., Houziaux L., Carnochan D.J., Wilson R., 1978, Catalogue of stellar ultraviolet fluxes, The Science Research Council, U.K.
- Turcotte S., Charbonneau P., 1993, ApJ 413, 376
- Venn K.A., Lambert D.L., 1990, ApJ 363, 234
- Van Winckel H., Mathias J.S., Waelkens C., 1992, Nat 356, 500
- Willmarth D., Barnes J., 1994, A User’s Guide to Reducing Echelle Spectra with IRAF, NOAO